

Blends of a Perfluorosulfonate Ionomer with Poly(vinylidene fluoride): Effect of Counterion Type on Phase Separation and Crystal Morphology

Forrest A. Landis and Robert B. Moore*

Department of Polymer Science, University of Southern Mississippi, P.O. Box 10076, Hattiesburg, Mississippi 39406-0076

Received April 11, 2000; Revised Manuscript Received June 13, 2000

ABSTRACT: The type of counterion present in the Nafion component of a blend with poly(vinylidene fluoride) (PVDF) is shown to affect phase separation and the crystalline polymorphism of the PVDF component. Nafion neutralized with an alkali metal counterion, Na^+ , results in blends displaying large-scale phase separation upon heating to temperatures above the melting point of PVDF. In contrast, when the Nafion counterion is changed to a larger tetrabutylammonium counterion (TBA^+), the melt is homogeneous, and with the exception of the PVDF crystallites, large-scale phase separation is not observed after the blend is cooled to room temperature. For the blends containing Na^+ -form Nafion, the crystalline morphology of the PVDF component develops in predominately the α crystal form, similar to pure PVDF crystallized from the melt. However, for blends containing TBA^+ -form Nafion, the PVDF component crystallizes with a higher content of the β - and/or γ -crystal forms. This effect of counterion type on the phase separation behavior and crystal morphology is attributed to the strength of the electrostatic cross-links within the Nafion component. Strong electrostatic cross-links induce gelation of the Nafion component leading to phase separation at elevated temperatures, whereas weak electrostatic cross-links provide a free-flowing melt that allows for a more favorable mixing with the PVDF component and is thus capable of influencing the crystallization process.

Introduction

In recent years, a wide variety of polymer blends have been developed to produce materials with enhanced chemical and physical properties. It is generally accepted that intermediate physical properties of a blend can be more readily controlled and optimized if the blend components are miscible (i.e., the polymer chains are intimately mixed on the molecular level as a result of favorable thermodynamic interactions). Because of the low entropy of mixing in polymer blend systems, miscibility is generally governed by enthalpic interactions between specific functional groups along the polymer chains. These specific molecular interactions, such as dipole–dipole, ion–dipole, and hydrogen-bonding interactions, have been widely employed to enhance the miscibility between dissimilar polymers.^{1–3}

One polymer that has been extensively studied in blend systems is poly(vinylidene fluoride) (PVDF). PVDF is a semicrystalline polymer that has been shown to be miscible with several common polar polymers that contain ester functional groups, including poly(1,4-butylene adipate),⁴ poly(vinyl esters),⁵ and poly(alkyl acrylates).^{6–8} The origin of miscibility between PVDF and these polar polymers has been attributed to strong dipole–dipole interactions between the polar carbon–fluorine bonds in PVDF and the carbonyl groups of the ester-containing polymers. The favorable molecular interactions in blends of PVDF and poly(methyl methacrylate) result in a significant melting point depression of the PVDF component of the blend. Nishi and Wang utilized this phenomenon to develop a method to determine the Flory–Huggins interaction parameter (χ_{12}) in semicrystalline polymer blend systems.⁷ The apparent miscibility of PVDF with acrylate polymers such as poly(methyl methacrylate) has also been shown to influence the chain conformation in the crystallites of PVDF.⁹

In addition to polymers containing carbonyl functionality, PVDF has been blended with ion-containing polymers, known as ionomers.^{10–12} Ionomers are a class of copolymers, which contain less than ca. 15 mol % of ionic repeat units distributed along the polymer backbone. Because of strong Coulombic forces involved with the anion/cation pairs, the ionic groups in an ionomer tend to aggregate into ionic domains, termed multiplets.¹³ These ionic structures have been shown to act as strong electrostatic cross-links and enhance the mechanical properties of the polymer.^{14–17} The improvement in mechanical properties of the ionomer is related to the strength of the electrostatic cross-links which can be varied by changing the size and type of counterion present in the ionomer.^{18,19}

One perfluorosulfonate ionomer, known as Nafion, has been the focus of a significant number of research studies.²⁰ The Nafion PFSI consists of a poly(tetrafluoroethylene) backbone with randomly distributed, sulfonate terminated, perfluoroether side chains. The strength of the electrostatic cross-links in Nafion has been shown to be greatly affected by varying the cationic counterions from small, alkali metal ions to large, quaternary alkylammonium ions.^{21,22} Specifically, tetrabutylammonium (TBA^+) counterions have been shown to greatly reduce the strength of Coulombic interactions in Nafion relative to the sodium neutralized form. This reduction in the strength of the ionic cross-links results in an increase in the mobility of ionomer chains at elevated temperatures, thereby allowing for Nafion to be melt processed.¹⁸

In previous studies, Kyu and co-workers examined the blend system of PVDF and Nafion in the acid and sodium neutralized forms.^{10–12} The results of these studies suggested that this blend system was partially miscible below the crystalline melting point of the PVDF component; however, upon heating above the melt transition temperature, liquid–liquid phase separation

occurred. Furthermore, it was shown that the blend composition and solvent-casting technique had a significant effect on the spherulitic morphology of PVDF in the blend. On the basis of our recent rheological studies of Nafion,^{18,21} the phase separation observed in PVDF/Nafion blends at elevated temperatures could be attributed to the difference in melt viscosity between the relatively fluid PVDF and the dynamically cross-linked Nafion component. In this investigation, we examine the effect of counterion type on the phase separation behavior of blends of PVDF with Nafion in the Na⁺ and TBA⁺ neutralized forms. In addition, we evaluate the manner in which the strength of the electrostatic cross-links in Nafion affects the crystalline morphology of the PVDF component in the blend.

Experimental Section

Materials. Poly(vinylidene fluoride) (Kynar 741, M_w = 154 000 g/mol) was obtained from Elf Atochem North America, Inc. Nafion 117 (1100 equivalent weight, sulfonic acid form) was provided by E.I. DuPont de Nemours & Co. Tetrabutylammonium hydroxide and sodium hydroxide were obtained from Aldrich Chemical Co. and used without further purification.

Preparation of Nafion/PVDF Blends. A soluble powder of Na⁺-form Nafion was prepared using a casting technique while a soluble powder of TBA⁺-form Nafion was prepared using a previously described steam stripping process.¹⁸ These procedures first involved refluxing the as-received Nafion films in an 8 M methanolic H₂SO₄ solution for 1 h to ensure complete conversion of the ionomer to the acid form. The films were then washed several times with deionized water to remove excess acid prior to being refluxed for 1 h in a 1 M TBAOH or NaOH solution in 50/50 methanol/water. Using a Parr reactor, the neutralized ionomer films were dissolved at 250 °C and 1400 psi in a 50/50 ethanol/H₂O solution for Na⁺-form Nafion and 45/5/50 ethanol/2-propanol/H₂O solution for TBA⁺-form Nafion. The TBA⁺-form Nafion was recovered by slowly dripping the ionomer solution into boiling water. As the organic alcohols rapidly boiled out of the solution, the Nafion precipitated and was easily claimed as a fluffy, white solid. A solvent casting technique was used to recover the Na⁺-form Nafion from the solution. This process involved pouring a small amount of the solution onto a hot crystallizing dish, which rapidly flashed off the solvents and left a solid polymer residue. Both Na⁺- and TBA⁺-form Nafion solids were dried for 24 h in a vacuum oven at 100 °C and then ground into a fine powder. Using these techniques, the resulting Nafion samples were amorphous and readily soluble in solvents such as *N,N*-dimethylacetamide and dimethyl sulfoxide.

Solution blends of the ionomer with PVDF were prepared by combining the solid powders together in the proper weight fractions and dissolving in a 40/60 *N,N*-dimethylacetamide (DMA)/acetone solution at a concentration of 0.004 g/mL. Films of the polymer blends were then prepared by two methods. Thin films (~10 μm in thickness) for optical microscopy, infrared spectroscopy, and small-angle laser light scattering studies were prepared by casting the solutions onto glass slides at 130 °C, followed by vacuum-drying at 80 °C for 24 h. Thicker films (~150 μm) for DSC and X-ray analysis were prepared by evaporating ca. 5 mL of the polymer blend solutions in 20 mL glass vials in an oil bath at 130 °C, followed by vacuum-drying the resulting films for 24 h in a vacuum oven at 80 °C.

Microscopic Methods of Blend Characterization. The blend morphologies of the cast films in the melt phase were characterized using a Nikon Optiphot2 polarizing optical microscope with an attached Mettler FP82HT hot stage with the analyzing polarizer removed. The cast films were heated to 240 °C to allow for complete melting of the PVDF crystallites. Electron micrographs of the phase morphology of the Nafion/PVDF blends were obtained using an Electroscan environmental scanning electron microscope (ESEM). The

thick cast films were heated to 240 °C for 5 min to allow for possible liquid/liquid phase separation, rapidly quenched in liquid nitrogen, and then fractured prior to imaging the fracture surface using ESEM analysis.

Scattering Methods of Blend Characterization. The effect of counterion type on the phase separation behavior of the polymer blends was examined using a small-angle laser light scattering (SALS) apparatus similar to that described by Stein and Rhodes.^{10,11,23} The incident light was produced from a 3 mW He-Ne laser (Oriel Corp., model 6697), and the scattered V_v patterns were recorded on Polaroid type 55 film. The thin blend films were analyzed at various temperatures using a Mettler FP82HT hot stage.

Using a Siemens XPD-700P polymer diffraction system equipped with a two-dimensional, position sensitive area detector and a sample-to-detector-distance of 49 cm, small-angle X-ray scattering patterns (SAXS) were obtained to further probe the morphology of cast and melt-treated Nafion/PVDF blends. Because of the similar electron density of the Na⁺ ionic domains in Nafion and the fluorocarbon polymer matrix, the blends containing Na⁺-form Nafion were refluxed in boiling water for 1 h to increase the scattering contrast.²⁴ The films were examined in the as-cast state and after heating to 220 °C to allow for enhanced ionic aggregation. High-temperature SAXS was performed on the Siemens diffraction system with a Mettler FP82HT hot stage inserted into the beam path. Scattering profiles were obtained during a 1 h exposure time. No significant degradation of the Nafion/PVDF blends was observed.

Characterization of the Crystal Morphology of PVDF. The thermal properties of the Nafion/PVDF blends were examined using a Perkin Elmer DSC 7. The DSC samples were heated under a N₂ atmosphere through the crystalline melting range of PVDF and held at 220 °C for 5 min in order to eliminate thermal history and the effects of persistent crystalline nuclei. These samples were then cooled at a rate of 200 °C/min to an isothermal crystallization temperature of 145 °C. After a period of 1 h at the isothermal crystallization temperature, the samples were scanned at a rate of 20 °C/min, through the crystalline melting range of PVDF to a temperature of 220 °C. The spherulitic superstructure of the PVDF crystalline domains was examined using a Nikon Optiphot2 polarizing optical microscope with an attached Mettler FP82HT hot stage. The films were held in the melt (220 °C) for 5 min to allow for complete melting of the PVDF crystallites and then rapidly cooled to a crystallization temperature of 150 °C.

Infrared spectroscopic analysis of the Nafion/PVDF films was performed on a Nicolet Protégé 8000 spectrometer to determine the effect of Nafion counterion type on the polymeric crystal structures of the PVDF component in the blends. Samples for FTIR analysis were conditioned in the Mettler FP82HT hot stage at 220 °C for 5 min to allow for complete melting of the PVDF crystallites and then rapidly cooled to a crystallization temperature of 150 °C. The polymeric nature of the crystal structures of PVDF in the blends was also examined by wide-angle X-ray diffraction (WAXD) using a Siemens XPD-700P polymer diffraction system equipped with a two-dimensional, position sensitive area detector. A sealed tube source was used to produce the Cu K α radiation (λ = 0.154 nm), and the sample-to-detector distance was set at 10 cm. The WAXD samples were heated in the Mettler FP82HT hot stage to 220 °C for 5 min and rapidly cooled to a crystallization temperature of 150 °C.

Information on the spherulitic growth of the Nafion/PVDF blends was obtained using a Nikon Optiphot2 polarizing optical microscope with an attached Mettler FP82HT hot stage. Thin films were cast on glass slides, heated to the melt at 220 °C for 5 min, and then rapidly cooled to isothermal crystallization temperatures in the range of 146–154 °C. Using a video attachment for the microscope that allows the images to be captured and saved on a computer, the size of the spherulites was determined from the image files by measuring the diameter of the spherulites using the SigmaScan image analysis software package. The size of the spherulites at each crystallization temperature was determined as a function of

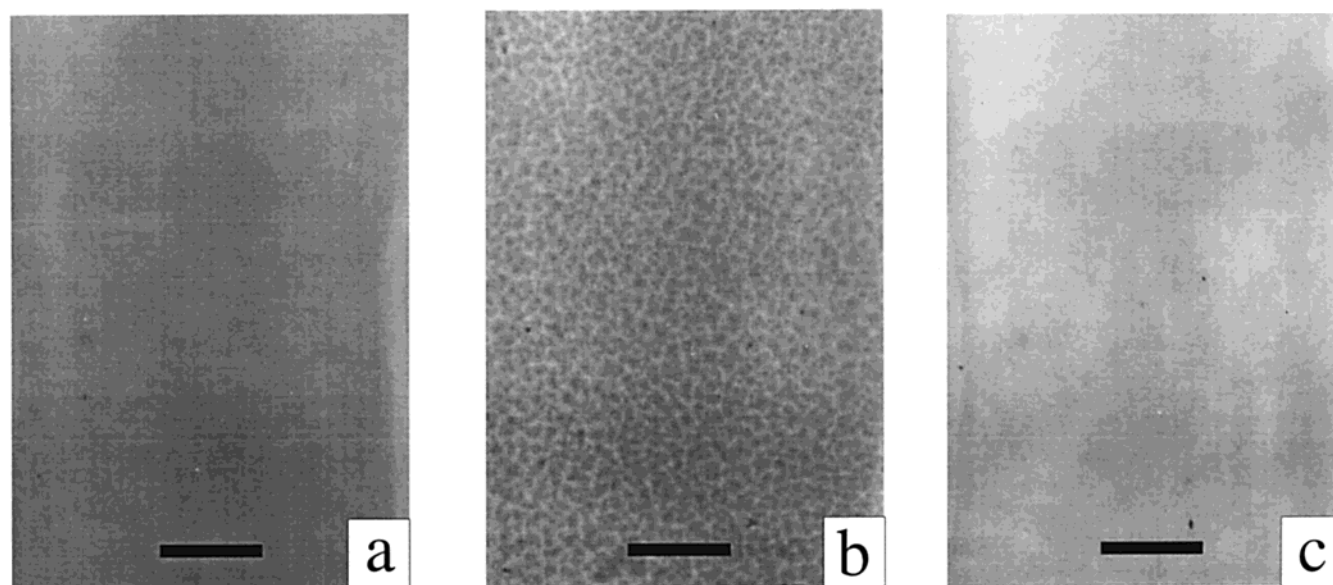


Figure 1. Optical micrographs in the melt at 220 °C of (a) PVDF, (b) 40/60 Na⁺-form Nafion/PVDF, and (c) 40/60 TBA⁺-form Nafion/PVDF. (Scale bar represents 100 μm.)

time. Using linear regression analysis, the radial growth rate of the PVDF spherulites was calculated from the average growth rate of three individual spherulites.

Results and Discussion

Effect of Counterion Type on the Phase Separation Behavior of Nafion/PVDF Blends. The effect of counterion type on the phase behavior of Nafion/PVDF blends can be readily observed using optical and scanning electron microscopy. Figure 1 compares the morphology of pure PVDF to blends of PVDF with Na⁺- and TBA⁺-form Nafion in the melt state at 240 °C. The high-temperature micrographs of pure PVDF and blends of TBA⁺-form Nafion/PVDF (Figure 1a,c) are both featureless and indicate that the blend yields a homogeneous melt phase. In contrast to the optical micrograph of the TBA⁺-form blend, the blend of PVDF with Na⁺-form Nafion (Figure 1b) displays a coarse, inhomogeneous morphology, indicative of a phase-separated system. Figure 2 displays the freeze-fractured surface topography of 40/60 Na⁺- and TBA⁺-form Nafion/PVDF blends, which were heated to 240 °C and rapidly quenched in liquid nitrogen. In agreement with the optical microscopy data, the Na⁺-form Nafion blend exhibited a coarse fracture surface, suggesting an immiscible blend system while the surface of the TBA⁺-form Nafion blend was smooth and homogeneous, suggesting a melt-miscible blend. These data clearly demonstrate that the choice of counterion significantly affects the extent of phase separation in Nafion/PVDF blends at elevated temperatures. Moreover, the ESEM data confirm that the homogeneous texture observed in the optical micrographs of the TBA⁺-form blends is a result of a uniformly mixed system and not simply an artifact of poor optical contrast.

The distinct effect of counterion type on phase separation is not limited to the melt state. For example, when 40/60 blends of Nafion and PVDF were cast from solution, the resulting thin films (i.e., less than 10 μm) were optically transparent regardless of the counterion type and visually resembled comparably thin films of pure PVDF. Upon heating the blended films above the melt point of the PVDF component, the blends contain-

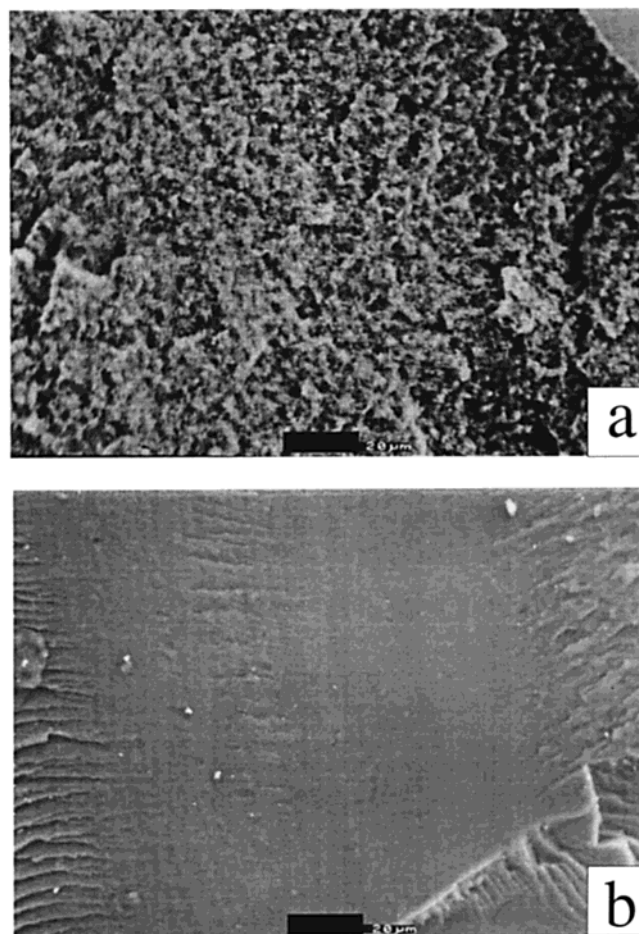


Figure 2. Freeze-fractured electron micrographs of blends of (a) 40/60 Na⁺-form Nafion/PVDF and (b) 40/60 TBA⁺-form Nafion/PVDF. (Scale bar represents 20 μm.)

ing Na⁺-form Nafion became visibly translucent. Moreover, this translucence persisted upon cooling the films to room temperature. As with most polymer blends, opacity (i.e., cloud-point behavior) is generally considered to be indicative of a phase-separated morphology

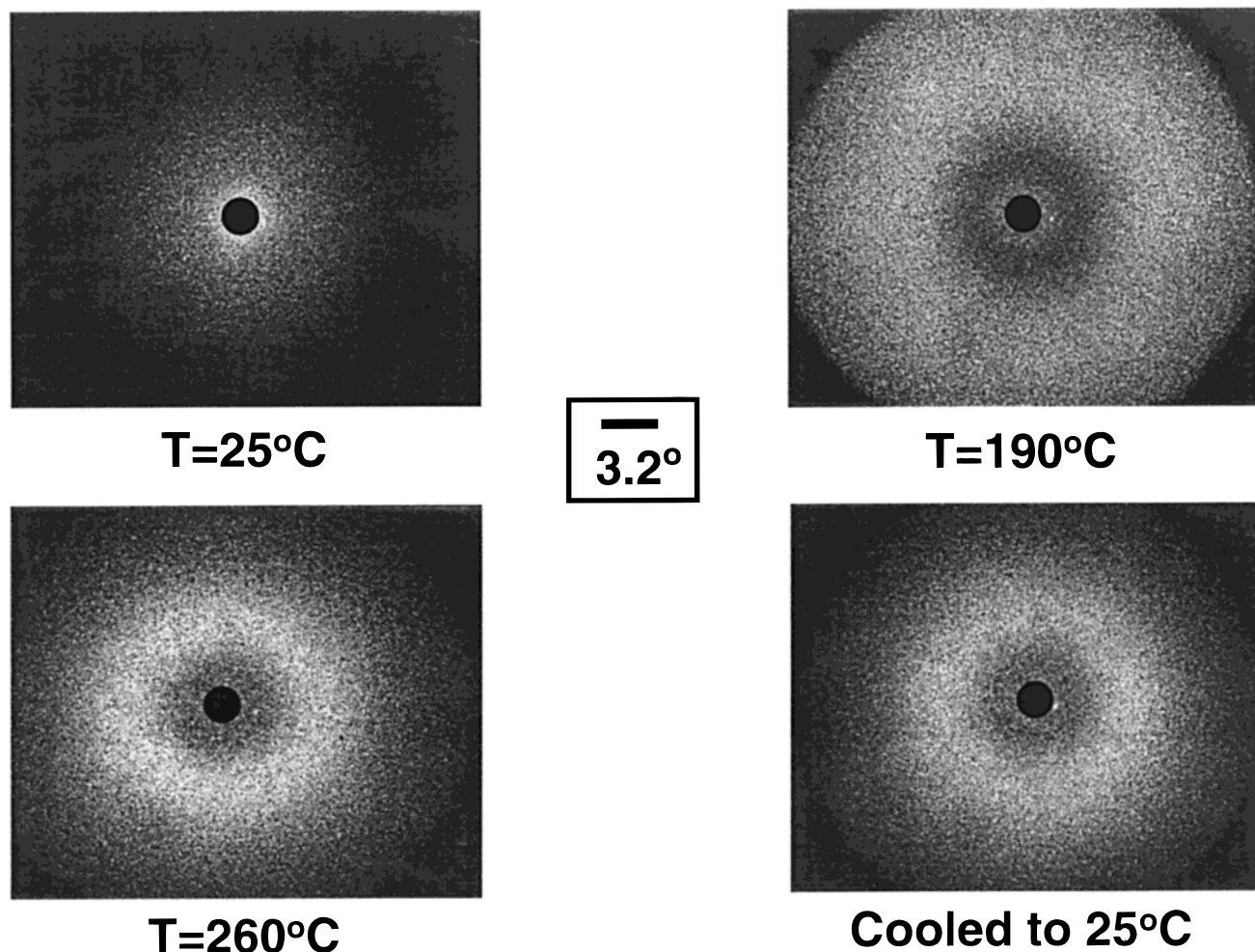


Figure 3. Small-angle laser light scattering patterns of 40/60 Na⁺-form Nafion with PVDF as a function of temperature (V_v polarizer orientation).

and is attributed to the scattering of light from the immiscible blend domains having distinctly different refractive indices. In contrast to the Na⁺-form blend, however, the TBA⁺-form blend and the control film of pure PVDF remained relatively transparent throughout the entire heating/cooling process.

The observed difference in clarity of the films upon heating was further examined using small-angle light scattering. Previous SALS analysis performed by Kyu and Yang on acid form Nafion blends with PVDF^{10–12} showed that, immediately above the melting point of PVDF, a halo in the SALS pattern developed which was attributed to phase separation of the blend components consistent with the latter stages of spinodal decomposition. Similar analysis of 60 wt % Na⁺- and TBA⁺-form Nafion blends with PVDF is shown in Figures 3 and 4.

For the as-cast Na⁺-form blend at room temperature (Figure 3), only minimal scattering was observed in the SALS patterns due to the crystallites of PVDF and minor surface imperfections resulting from the casting process. As the sample was heated to a temperature above the melting point of the PVDF component in the blend (190 °C), a scattering halo developed, indicating liquid–liquid phase separation of the dissimilar polymers. Upon further heating to 260 °C, the scattering halo increased in intensity and moved to smaller scattering angles, implying that the dimensions of the phase-separated domains were becoming larger (i.e., a phase coarsening process). When the Na⁺-form Nafion

blend was cooled back to room temperature, the scattering halo persisted; however, a slight decrease in scattering intensity was observed. This scattering behavior is comparable to that reported by Kyu and Yang.¹¹

When a similar heating cycle was applied to the TBA⁺-form blend (Figure 4), the sample exhibited an identical SALS scattering pattern to the Na⁺-form blend in the as-cast state. In dramatic contrast to the Na⁺-form Nafion blend with PVDF, the TBA⁺-form Nafion blend exhibited a featureless scattering profile with no evidence of a halo up to a temperature of 260 °C. This absence of scattering in the SALS patterns is in agreement with the optical micrographic data (Figure 1) and further demonstrates that, at least in the melt, TBA⁺-form Nafion yields a more homogeneous blend with PVDF, relative to Na⁺-form Nafion. On the size scale probed by the optical and electron microscopic methods, it is apparent that Na⁺-form Nafion is immiscible with PVDF and yields phase-separated domains with dimensions on the order of micrometers. In contrast, the phase dimensions in the TBA⁺-form Nafion blends with PVDF (if present) are on a size scale below that which can be resolved using these morphological techniques (i.e., smaller than the wavelength of visible light).

While the characterization methods described to this point are useful for qualitatively evaluating large-scale phase separation in polymer blends, it is important to note that the issue of potential blend miscibility is quite

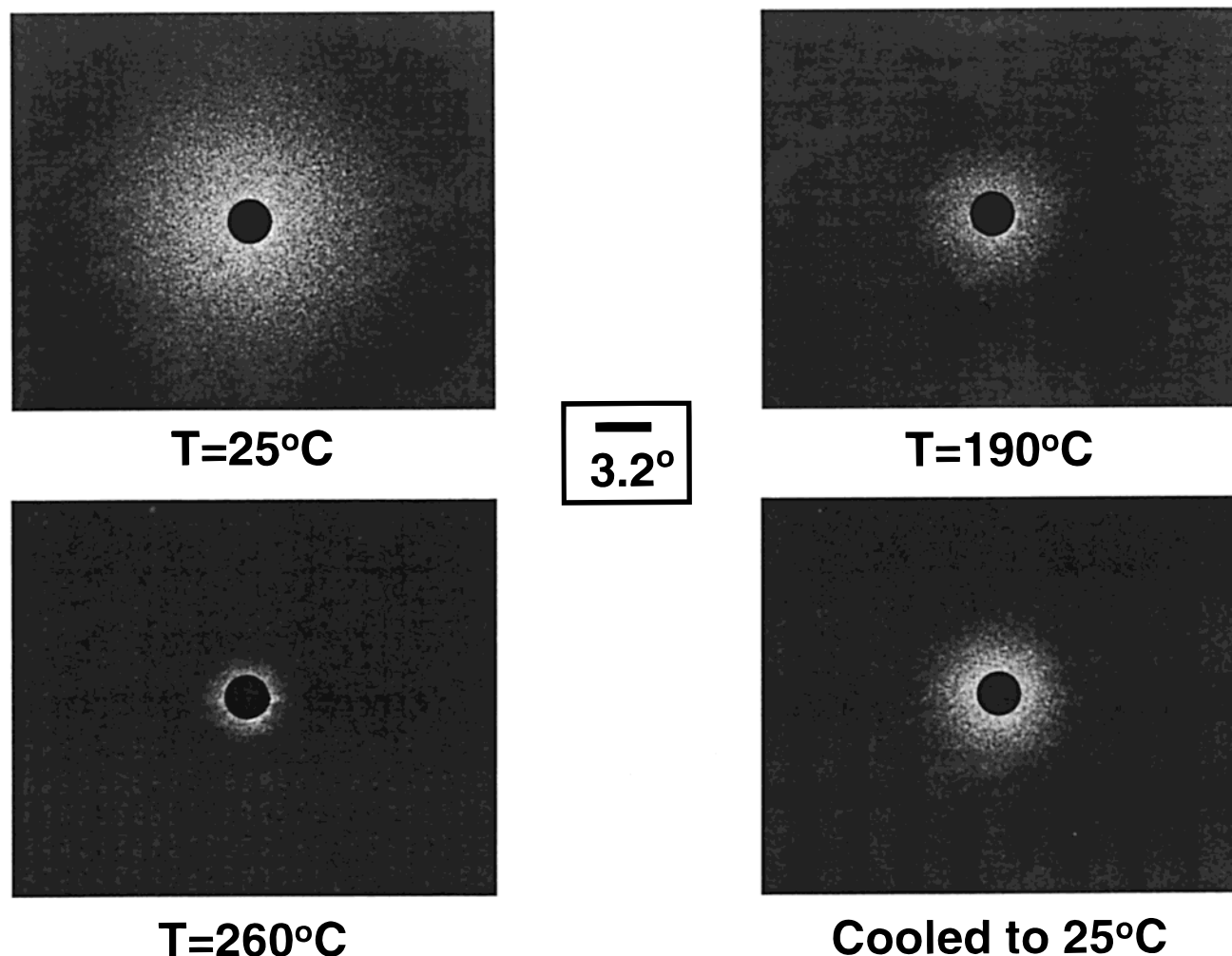


Figure 4. Small-angle laser light scattering patterns of 40/60 TBA⁺-form Nafion with PVDF as a function of temperature (V_v polarizer orientation).

complex with respect to the dimensions of the phase-separated domains. Although the phase behavior of Nafion/PVDF blends is clearly different when the ionomer counterion is varied from Na⁺ to TBA⁺, the Nafion component of both blend systems still displays a strong tendency toward ionic aggregation, as evidenced by the SAXS profiles of the blends in Figure 5. The Na⁺- and TBA⁺-form Nafion blends with PVDF exhibit scattering maxima at $q_{\max} = 1.4$ and 2.0 nm^{-1} , respectively, which have been attributed to interparticle scattering from the ionic aggregates with an interaggregate distance on the order of 3–4 nm.²⁴ Since the q_{\max} of the “ionomer peaks” is identical to that observed with the pure ionomers, it is reasonable to conclude that the PVDF component does not significantly pervade the ionic domains or appreciably disrupt ionic aggregation. This behavior is in contrast to that typically observed for *miscible* ionomer blends (e.g., sulfonated polystyrene and nylon-6), whereby strong specific interactions involving the ionic groups preclude ionic aggregation.^{25,26}

The presence of ionic aggregation in blend systems which appear to be otherwise completely miscible has been reported by Register and co-workers for blend systems of sulfonated polystyrene (SPS) and poly(2,6-dimethyl-1,4-phenylene oxide) (PXE).^{27,28} In this system, it was determined that the type of counterion in SPS greatly influenced the blend miscibility with PXE. Na⁺-neutralized SPS exhibited the highest immiscibility

with PXE, while Zn²⁺-neutralized SPS yielded the highest blend miscibility. This difference in blend miscibility as the counterion is varied was explained by considering the relative strength of interaction of sodium sulfonate groups compared to zinc sulfonate groups. Na⁺ ions produce relatively strong ion pair associations because of their greater ionic binding nature while Zn²⁺ ions have a significantly greater covalent character and form weaker ion pair associations. This difference in the strength of ionic interactions manifests itself in a significantly higher melt viscosity for Na⁺-form SPS relative to Zn²⁺-form SPS. With weaker ionic associations, the morphology of the ionic domains in the Zn²⁺-form SPS ionomer is more easily disrupted by the presence of PXE, yielding smaller aggregates and/or more ionic groups dispersed in the matrix. The disruption of the ionic aggregates results in a greater accommodation of the PXE component and a more intimate mixture of the PXE and SPS chains (i.e., “greater miscibility”) relative to the Na⁺-form SPS blend.

In contrast to the inherent miscibility of PS and PXE backbones of the blend system studied by Register, it is unlikely that the backbones of Nafion (i.e., PTFE) and PVDF are miscible. Nevertheless, a similar explanation for the effect of counterion type on phase behavior can be realized in the Nafion/PVDF system. The strongly interacting Na⁺-form Nafion yields a stable electrostatic network that effectively “gels” the Nafion-rich phase and

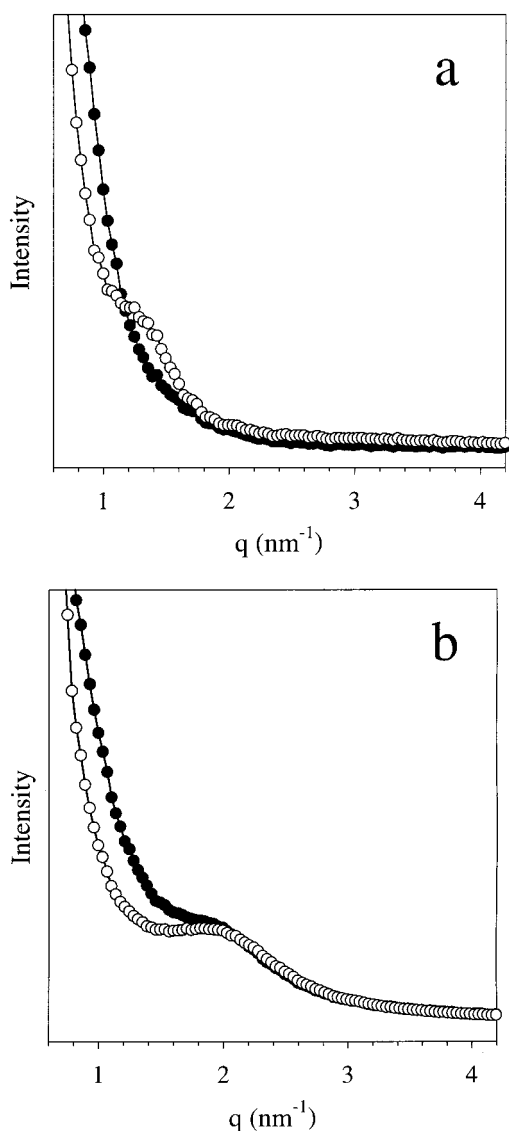


Figure 5. Small-angle X-ray scattering profiles observed at room temperature of 60/40 Nafion/PVDF blends: (a) Na⁺-form as cast (●) and after heating to 220 °C (○); (b) TBA⁺-form as cast (●) and after heating to 220 °C (○).

thus exhibits immiscibility with PVDF. On the other hand, the electrostatic network in the much weaker associating TBA⁺-form Nafion is more easily destabilized (particularly at elevated temperatures)^{18,22} and thus exhibits an apparent single-phase behavior characteristic of a melt-miscible blend.

The effect of thermal treatment is also shown to have a significant effect on the small-angle X-ray scattering behavior of the blends. In the SAXS profiles of Figure 5, the ionomer peak is clearly absent for the as-cast Na⁺-form Nafion/PVDF blend, while a broad shoulder is evident for the as-cast TBA⁺-form blend. After heating the as-cast samples to a temperature of 220 °C (i.e., above the melting point of the PVDF component), the ionomer peak becomes more distinct, and the small-angle upturn shifts to lower angles, for *both* blends. These data suggest that the state of ionic aggregation in the Nafion/PVDF blends is poorly developed in the as-cast state and becomes enhanced after the blends are annealed above the melting point of the PVDF component.

Previous SAXS studies of SPS films cast from a THF/water solution have shown that the ion pairs did not associate into large ionic aggregates as evidenced by an absence of a characteristic SAXS ionomer peak.²⁹ This state of ionic dispersion was likely facilitated by the ionic solvation effect of the polar solvents used to cast the film and the low casting temperatures. Upon heating the as-cast SPS sample to temperatures above ca. 165 °C, an ionomer peak developed and increased in intensity with increasing temperature. An analogous effect of solvent casting and thermal treatment on the morphology of sulfonated polystyrene ionomers is also observed in the Nafion/PVDF blends.

For the as-cast, Na⁺-form Nafion blend, the polar sodium sulfonate ion pairs are apparently dispersed in the matrix as very small aggregates and/or lone pairs, which do not provide sufficient scattering contrast to yield an ionomer peak. As the casting solvent is evaporated during the final stages of film formation, these small aggregates effectively hinder chain mobility and thus the formation of larger aggregates. Once the blend has been subjected to elevated temperatures, however, the increased molecular mobility in the melt allows for a redistribution of the ion pairs into larger ionic aggregates that, after cooling to room temperature, are of a sufficient size to yield an observable scattering maximum. For the TBA⁺-form Nafion blend, the electrostatic cross-links are weak and result in a relatively high mobility of the TBA⁺SO₃⁻ ion pairs at elevated temperatures.^{18,22} Therefore, in contrast to the behavior of the Na⁺-form blend, this increased mobility at the casting temperature results in the formation of relatively large aggregates that yield a discernible ionomer peak in the as-cast TBA⁺-form blend. After the thermal treatment (i.e., heating to 220 °C), the ion pairs in the TBA⁺-form blend simply organize into aggregates of greater definition and yield a more resolved SAXS maximum.

Although the state of ionic aggregation in the TBA⁺-form blends appears to be greater than that of the Na⁺-form system, the relative thermal stability of the electrostatic network in these blends is a key element in understanding the observed differences in phase behavior at elevated temperatures. Figure 6a compares the SAXS profiles of a TBA⁺-form Nafion/PVDF blend at room temperature to that of the same sample at 180 and 240 °C. In the initial room temperature profile, the ionomer peak is clearly observed. However, at 180 °C, the intensity of the ionomer peak is significantly diminished, and at 240 °C, the SAXS profile is essentially featureless. Once this heat-treated sample is cooled back to room temperature, the ionomer peak reappears. Note that identical scattering behavior is observed for a pure TBA⁺-form Nafion at elevated temperatures, as shown in Figure 6b. In contrast to the high-temperature scattering behavior of Nafion in the Cs⁺ form³⁰ and Ag⁺ form,²⁴ which clearly show that ionic aggregation persists at temperatures above the melting point, the data in Figure 6 suggest that the state of ionic aggregation in TBA⁺-form Nafion is significantly disrupted at elevated temperatures. This unusual scattering behavior for Nafion may be attributed to the weak Coulombic interactions between the large alkylammonium sulfonate ion pairs, which allow for rapid ion-hopping kinetics at high temperatures (i.e., the thermally activated process of ion pairs transferring from aggregate to aggregate in attempt to satisfy the local balance

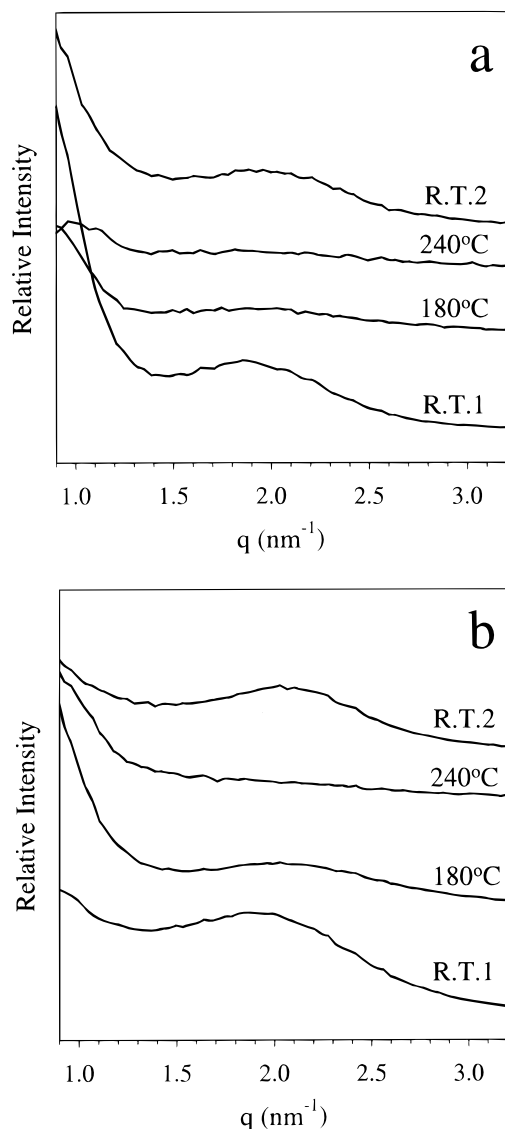


Figure 6. Small-angle X-ray analysis of Nafion/PVDF blends at elevated temperatures: (a) 60/40 TBA⁺-form Nafion/PVDF; (b) pure TBA⁺-form Nafion.

between electrostatic and elastic forces within the dynamic network).^{31,32} With high ion pair mobility, the local distribution of ion pairs becomes more homogeneous, and thus the global scattering contrast is lost.

In correlating the SAXS data in Figures 5 and 6 to the morphological information from the SALS and microscopy studies, it is apparent that the phase dimensions of the blend components in the original as-cast samples of the Na⁺-form and TBA⁺-form Nafion/PVDF blends are very small and homogeneously dispersed. At temperatures above the melting point of PVDF, however, the ionic groups attached to the ionomer become mobile and begin to form a more organized electrostatic network in the Nafion-rich domains. For the Na⁺-form Nafion/PVDF blend, the concentration fluctuations characteristic of spinodal decomposition¹² yield large, phase-separated domains of Nafion that become dimensionally stabilized by the strong electrostatic cross-links. Since the ionic aggregates in Na⁺-form Nafion are expected to persist at temperatures above 300 °C,^{24,30} the Nafion-rich domains essentially become gelled particles that are incapable of significant flow and remixing with the fluid PVDF component. Once this phase coarsening develops,

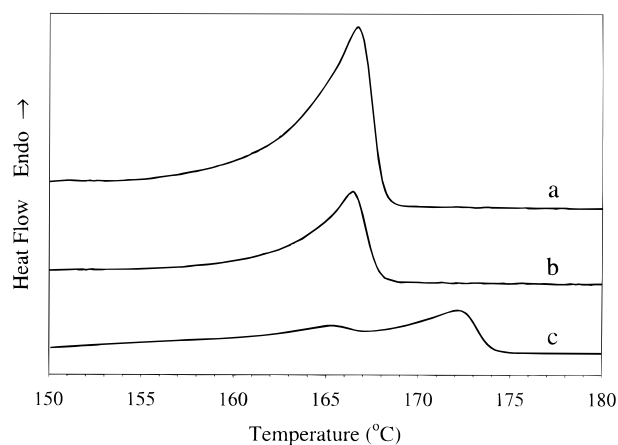


Figure 7. DSC thermograms of Nafion/PVDF blends crystallized from the melt at 145 °C: (a) pure PVDF, (b) 50/50 Na⁺-form Nafion/PVDF, and (c) 50/50 TBA⁺-form Nafion/PVDF.

the blend morphology is kinetically pinned³³ by the slow ion-hopping kinetics, and the observed phase-separation is, for all practical purposes, irreversible.

In contrast to the large-scale phase separation observed for the blends containing Na⁺-form Nafion, the TBA⁺-form Nafion/PVDF blends do not exhibit spinodal decomposition in the range of temperatures studied here. This behavior is attributed to the weak electrostatic interactions between the TBA⁺SO₃⁻ ion pairs and the relatively fast ion-hopping kinetics. At temperatures above the melting point of PVDF, the mobile ions in the TBA⁺-form Nafion domains yield a very dynamic network that allows for significant flow of the ionomer chains.¹⁸ This apparent enhancement in the rheology of the ionomer eliminates gelation, offers a closer viscosity match between the blend components, and thus allows for a more favorable mixing with the fluid PVDF domains.

Effect of Nafion Counterion Type on the Crystallization of PVDF. PVDF is known to crystallize in several different crystal polymorphs (i.e., α , β , γ , and δ)^{34–37} of which one of these structures, the β -form, is known to exhibit unique piezo-³⁸ and pyroelectric^{39,40} properties. Since the α - and γ -crystal forms are the most commonly observed polymorphs when PVDF is crystallized from the melt, an extensive amount of research has been conducted into various methods to produce the β -form of PVDF including techniques involving mechanical drawing,^{34,41,42} crystallization from specific solvents,⁴³ crystallization from the melt under high pressure,^{44,45} epitaxial growth on a KBr substrate,⁴⁶ and poling in high electric fields.⁴⁷ The polymorphic composition of PVDF in the β -form has also been shown to increase in blends of PVDF with other polymers such as PMMA.⁹

Multiple melting endotherms have been observed in the DSC thermograms of PVDF and attributed to the existence of different polymorphic crystal structures.^{44,48,49} Thus, DSC analysis may be used as a method to examine the thermal transitions that occur in the Nafion/PVDF blend systems and, more importantly, to evaluate the effect of the Nafion component on the polymorphic composition of PVDF in the blends. Figure 7 contains DSC thermograms of 50/50 Nafion blends with PVDF that were isothermally crystallized from the melt at 145 °C. In pure PVDF, and in the blend of Na⁺-form Nafion with PVDF, only one endothermic transition at 166 °C is observed. This thermal response

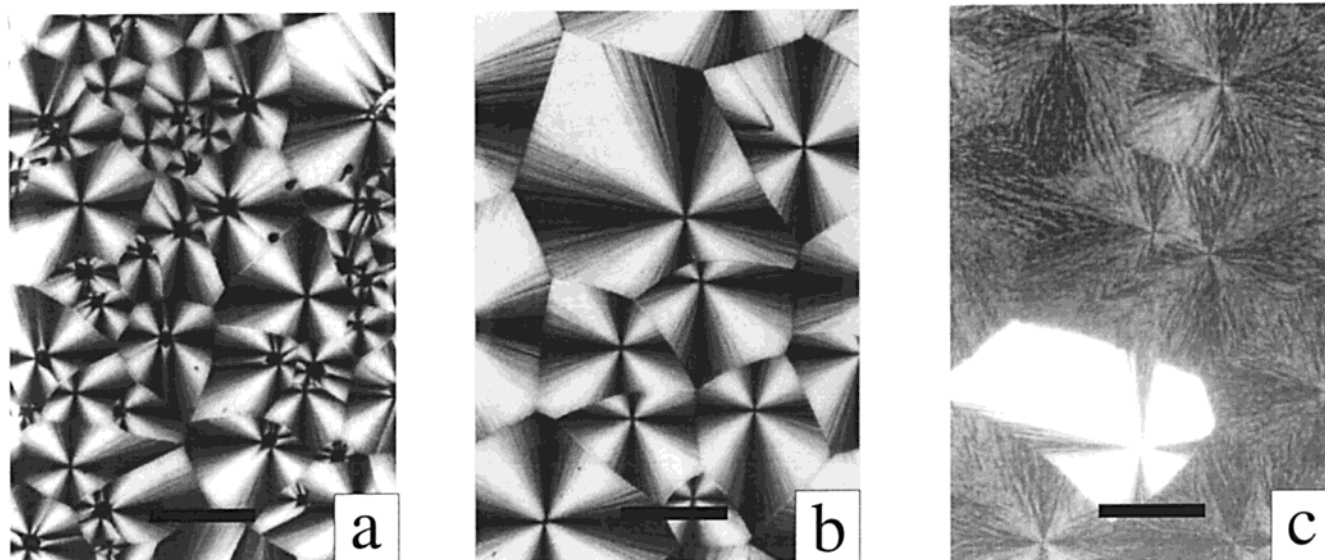


Figure 8. Polarized optical micrographs of Nafion/PVDF blends crystallized from the melt at 150 °C: (a) pure PVDF, (b) 10/90 Na⁺-form Nafion/PVDF, and (c) 10/90 TBA⁺-form Nafion/PVDF. (Scale bar represents 100 μm.)

suggests that the PVDF component in these blend systems consists primarily of one crystal polymorph (i.e., presumably the α -crystal structure). In contrast, when a blend of TBA⁺-form Nafion with PVDF is crystallized from the melt, two separate endothermic transitions are observed. One of these transitions occurs at 166 °C, which is consistent with the melting of the α -crystallites observed in pure PVDF. The second endotherm at 172 °C occurs at a higher temperature than the transition observed in pure PVDF, suggesting the presence of the higher melting β - or γ -crystal polymorphs. In addition to the appearance of a new higher temperature endotherm when PVDF is blended with TBA⁺-form Nafion, it should be noted that a slight melting point depression of the low-temperature endotherm is observed at these high Nafion blend compositions. In agreement with the preceding morphological data, this observation is consistent with a moderately favorable thermodynamic mixing of the two polymers in the melt state.⁷

In addition to DSC thermal analysis, polarized optical micrographs (Figure 8) were obtained for 10/90 Nafion/PVDF blends that were cooled from the melt to a crystallization temperature of 150 °C. The micrographs of pure PVDF and the blend with Na⁺-form Nafion exhibit large, well-formed spherulites with high birefringence similar to the α -crystal form spherulites described by Prest and Luca.⁵⁰ Conversely, the micrograph of the blend containing TBA⁺-form Nafion consisted primarily of large spherulites with much lower birefringence. These dim spherulites are similar in optical character to that of PVDF spherulites crystallized in the γ -form. With low Nafion contents in the blend, a few, very bright, α -form spherulites may be occasionally observed in the sample, as shown in Figure 8c. This morphology is in agreement with the observation of a small, low-temperature endotherm in the thermogram of the TBA⁺-form Nafion/PVDF blend (Figure 7, scan C).

To provide spectroscopic evidence for the ability of TBA⁺-form Nafion to influence the crystal morphology of PVDF, FTIR analysis of blends of Na⁺- and TBA⁺-form Nafion with PVDF was performed. The infrared bands at 795, 764, 615, and 530 cm⁻¹ have been attributed to the α -form of PVDF, while the bands at

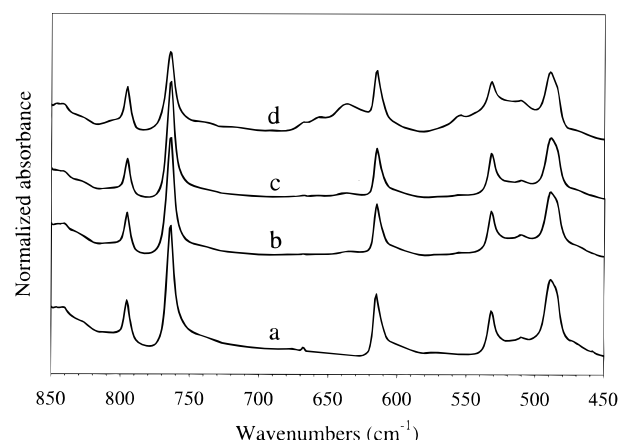


Figure 9. Infrared spectra of Na⁺-form Nafion/PVDF blends as a function of blend composition: (a) PVDF, (b) 10/90 Nafion/PVDF, (c) 20/80 Nafion/PVDF, and (d) 50/50 Nafion/PVDF.

840 and 510 cm⁻¹ have been attributed to the all-trans conformations of the β - and γ -forms.^{51,52} In addition, the band at 810 cm⁻¹ and the large absorption at 490 cm⁻¹ have been attributed to the γ -crystal form (the band at 490 cm⁻¹ also contains contributions from the amorphous PVDF component).^{49,53,54} Figures 9 and 10 are FTIR spectra of blends of Nafion with PVDF as the concentration of the ionomer and the counterion type are varied. The spectra in Figure 9 indicate that, as the amount of Na⁺-form Nafion is increased in the blend, there is little variation in the relative intensity of the vibrational bands of the crystal polymorphs in comparison to pure PVDF. In contrast, the spectra of the TBA⁺-form Nafion blends with PVDF (Figure 10) clearly show, with increasing Nafion content, an increase in the intensity of the vibrational bands at 840, 810, and 510 cm⁻¹ attributed to the β - and γ -form crystals. Concurrently, a decrease is observed in the intensity of the bands at 764, 615, and 530 cm⁻¹ attributed to the α -form crystals. This spectroscopic evidence indicates that the crystalline morphology of PVDF is not influenced by the presence of Na⁺-form Nafion domains, while the TBA⁺-form Nafion demonstrates a strong propensity to alter the crystal morphology of PVDF.

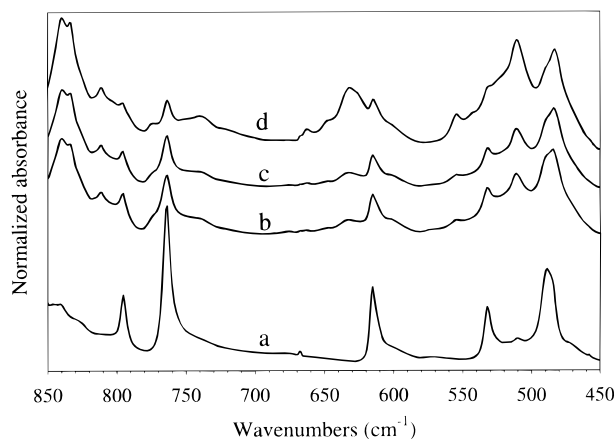


Figure 10. Infrared spectra of TBA⁺-form Nafion/PVDF blends as a function of blend composition: (a) PVDF, (b) 10/90 Nafion/PVDF, (c) 20/80 Nafion/PVDF, and (d) 50/50 Nafion/PVDF.

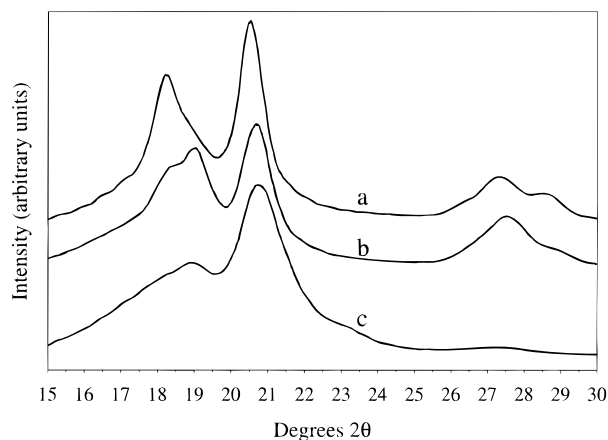


Figure 11. WAXD profiles of Nafion/PVDF blends crystallized from the melt at 150 °C: (a) PVDF, (b) 10/90 Na⁺-form Nafion/PVDF, and (c) 10/90 TBA⁺-form Nafion/PVDF.

WAXD analysis was utilized on blends that contained 10 wt % of the ionomer (Figure 11) in an effort to confirm the influence of TBA⁺-form Nafion on the crystal morphology of PVDF. While Nafion is known to have only a weak WAXD reflection at 18° 2θ due to the (100) plane of the crystalline PTFE backbone and an amorphous halo centered between ca. 2θ = 12°–20°,^{24,30,55} these features are not expected to significantly contribute to the diffractograms of the blends with PVDF due to the low level of crystallinity of Nafion and its low composition in the blend. The diffractogram of pure PVDF contains characteristic reflections due to the α-form crystallites, specifically the reflections due to the (110), (020), (100), and (120) crystal planes located at 27.0°, 20.4°, 18.8°, and 18.2° 2θ, respectively.^{56,57} A similar diffraction pattern is observed when PVDF is melt crystallized in the presence of Na⁺-form Nafion with the exception of a reflection at 2θ = 18.8° which may be attributed to the γ-crystal polymorph. In the blend of PVDF with TBA⁺-form Nafion, the characteristic reflections of the α-form at 27.0° 2θ have almost completely disappeared, and only two broad reflections at 18.8° and 20.5° are present. In agreement with the FTIR results, these reflections are more characteristic of a mixture of the γ- and β-polymorphic forms of PVDF.^{47,56,57}

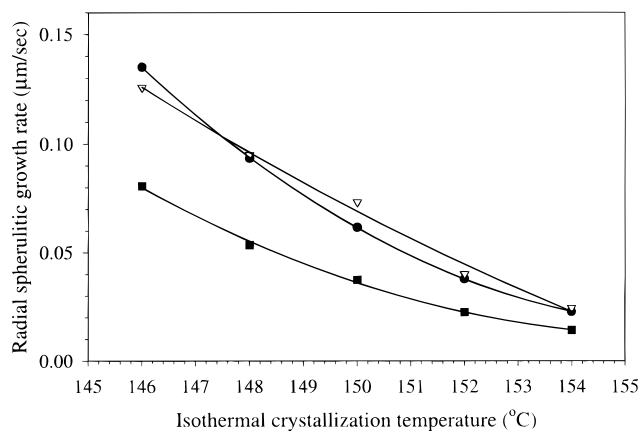


Figure 12. Spherulitic growth rate of 20/80 Nafion/PVDF blends: PVDF (●), Na⁺-form Nafion blend (▽), and TBA⁺-form Nafion blend (■).

With respect to the effect of these blends on the formation of polymorphic crystalline domains in the PVDF, previous studies have shown that melt crystallization of PVDF in the presence of PMMA can alter the crystal morphology of PVDF from the α-form to the β- or γ-crystal forms.⁹ While no satisfactory explanation was given for this phenomenon, it has been reported that the crystal growth rate of PVDF in the presence of PMMA is significantly reduced relative to that of pure PVDF.⁵⁸ Furthermore, it is known that when PVDF is crystallized at large supercoolings, the rapid crystallization yields the more kinetically favored α-crystal form.⁵⁹ As the temperature of crystallization approaches the melting temperature of PVDF, the rate of crystallization is significantly reduced, which may allow for the formation of the more thermodynamically favored β- and γ-crystal forms.

The effect of PMMA on the crystal morphology of PVDF may be explained by a diluent effect at the crystal growth front, which decreases the rate of crystallization in miscible PVDF/PMMA blends. To determine whether the presence of Nafion has a similar effect on the rate of crystallization of PVDF, isothermal spherulitic growth rates were obtained using optical microscopy. Figure 12 shows a comparison of the spherulitic growth rate of pure PVDF to 20/80 blends with Na⁺- and TBA⁺-form Nafion at various isothermal crystallization temperatures. These data demonstrate that the spherulitic growth rate of PVDF in the presence of Na⁺-form Nafion is nearly identical to the growth rate of pure PVDF. This result suggests that the Na⁺-form Nafion, which exhibits large-scale phase separation, cannot cause a significant decrease in the growth rate of the PVDF spherulites because the crystalline superstructures develop in isolated domains of pure PVDF. In contrast, the spherulitic growth rate of PVDF in the presence of TBA⁺-form Nafion is significantly reduced relative to that of pure PVDF. Furthermore, isothermal bulk crystallization of PVDF in blends with Nafion show that the crystallization half-times (*t*_{1/2}) at 147 °C for PVDF and a 20/80 Na⁺-form Nafion/PVDF blend are nearly identical at 2.64 and 2.82 min, respectively, while the *t*_{1/2} for a 20/80 TBA⁺-form Nafion blend increases to 6.31 min.⁶⁰ Clearly, the more melt-miscible TBA⁺-form Nafion can significantly perturb the crystallization of PVDF.

In the Nafion/PVDF blends examined in this study, the crystal growth front must reject the noncrystallizable Nafion component. The work of Martusceli and co-

workers has demonstrated that a reduction in the crystal growth rate of a crystallizable component in immiscible blends is strongly dependent on the size of the dispersed domains of the noncrystallizable component.⁶¹ For large, phase-separated domains, like that observed with Na⁺-form Nafion dispersed in PVDF, the growth of the PVDF crystallites will not be as significantly reduced relative to the crystal growth of PVDF in the presence of the more homogeneously dispersed TBA⁺-form Nafion. Therefore, it is reasonable to conclude that the reduced crystalline growth rate of PVDF in the presence of TBA⁺-form Nafion is an important factor in the ability of TBA⁺-form Nafion to alter the crystal morphology of PVDF and thus yield a greater composition of the thermodynamically favored γ - and β -crystal forms. Other contributions involving specific interactions between the PVDF and Nafion chains during the crystallization process are not ruled out; however, further investigations, beyond the scope of this study, will be required to fully understand this complex phenomenon.

Conclusions

Blends of poly(vinylidene fluoride) with Nafion containing Na⁺ and TBA⁺ counterions were prepared and evaluated for their phase behavior and the nature of the crystalline morphology of the PVDF component. Variation of the Nafion PFSI counterion from Na⁺ to TBA⁺ in blends with PVDF was found to have a significant effect on the extent of phase separation. Nafion neutralized with an alkali metal counterion, Na⁺, resulted in blends displaying large-scale phase separation upon heating to temperatures above the melting point of PVDF. This phase separation was found to be irreversible and persisted after the blends were cooled to room temperature. In contrast, when the Nafion counterion was changed to a larger tetrabutylammonium counterion (TBA⁺), optical microscopy and small-angle laser light scattering data showed that the melt was homogeneous, and with the exception of the PVDF crystallites, no evidence of phase separation was observed upon cooling the blend to room temperature. Although the microscopy and light scattering results suggested that, on the size scale probed by these techniques, blends of PVDF with Na⁺-form Nafion are immiscible while blends with TBA⁺-form Nafion are miscible, the small-angle X-ray scattering results indicated that in both blend systems the ionomer still exhibits ionic aggregation (i.e., nano-phase separation) with characteristic dimensions of the ionic domains identical to that of the pure ionomer.

The clearly observed immiscibility of Na⁺-form Nafion/PVDF blends is attributed to the strong Coulombic forces between the SO₃⁻-Na⁺ dipoles which lead to aggregation of the ion pairs into stable multiplets that act as strong electrostatic cross-links. These kinetically stable cross-links in the Na⁺-form Nafion have been shown to persist at temperatures well above the PVDF melting point and consequently induce gelation of the Nafion component leading to irreversible phase separation at elevated temperatures. In contrast, neutralization of the Nafion component with more weakly interacting TBA⁺ cations, significantly reduces the strength of the dynamic electrostatic network at elevated temperatures. With considerable ion hopping at temperatures above the PVDF melting point, the TBA⁺-form Nafion chains are much more mobile, relative to the

Na⁺-form Nafion chains. This enhanced mobility in the melt effectively eliminates the potential for gelation and thus provides a free-flowing melt that allows for a more favorable mixing with the PVDF component.

An additional effect of altering the phase behavior by changing the counterion in Nafion/PVDF blends is recognized in the crystalline morphology of the PVDF component when these blends are crystallized from the melt. When Na⁺-form Nafion blends with PVDF are melt-crystallized, the α -form crystal polymorph is predominately observed which is quite similar to that of pure PVDF crystallized under similar conditions. Conversely, optical microscopic and spectroscopic techniques indicate that a greater amount of the β - and γ -crystal polymorphs are observed when PVDF is crystallized in the presence of TBA⁺-form Nafion. The effect of the Nafion counterion type on the crystal morphology of PVDF may be explained by the apparent influence of the TBA⁺-form Nafion on the crystallization kinetics of PVDF, relative to that observed with the Na⁺-form Nafion. In the case of Na⁺-form Nafion blends with PVDF, the system is phase-separated into large domains that have little effect on the growth of the PVDF crystals within the isolated, pure PVDF domains. In contrast, the melt-miscible TBA⁺-form Nafion component consequently slows the crystal growth rate of PVDF, thereby allowing for the formation of the more thermodynamically favored β - and γ -crystal forms.

Acknowledgment. The authors acknowledge funding for this research by the National Science Foundation (Grants DMR-9211963 and INT-9730032), the Air Force Office of Scientific Research (Grant F49620-93-1-0189DEF), and the Mississippi NSF EPSCoR Program (Grant EPS-9874669). We also thank Professor K. Tashiro (Osaka University, Japan) for helpful discussions regarding the characterization of PVDF polymorphism.

References and Notes

- (1) Coleman, M. M.; Graf, J.; Painter, P. C. *Specific Interactions and the Miscibility of Polymer Blends: Practical Guides for Predicting and Designing Miscible Polymer Mixtures*; Technomic Publishing Co, Inc.: Lancaster, PA, 1991.
- (2) Utracki, L. A. *Polymer Alloys and Blends*; Hanser Publishers: New York, 1990.
- (3) Utracki, L. A.; Weiss, R. A., Eds.; *Multiphase Polymers: Blends and Ionomers*; American Chemical Society: Washington, DC, 1989; Vol. 395.
- (4) Penning, J. P.; St. J. Manley, R. *Macromolecules* **1996**, *29*, 77.
- (5) Bernstein, R. E.; Paul, D. R.; Barlow, J. W. *Polym. Eng. Sci.* **1978**, *18*, 683.
- (6) Noland, J. S.; Hsu, N. N. C.; Saxon, R.; Schmitt, J. M. *Adv. Chem. Ser.* **1971**, *99*, 15.
- (7) Nishi, T.; Wang, T. T. *Macromolecules* **1975**, *8*, 909.
- (8) Wahrhund, D. C.; Bernstein, R. E.; Barlow, J. W.; Paul, D. R. *Polym. Eng. Sci.* **1978**, *18*, 677.
- (9) Yang, D.; Thomas, E. J. *J. Mater. Sci. Lett.* **1987**, *6*, 593.
- (10) Yang, J. C. Ph.D. Dissertation, University of Akron, Akron, OH, 1989.
- (11) Kyu, T.; Yang, J. C. *Macromolecules* **1990**, *23*, 176.
- (12) Kyu, T.; Yang, J. C. *Macromolecules* **1990**, *23*, 182.
- (13) Eisenberg, A.; Hird, B.; Moore, R. B. *Macromolecules* **1990**, *23*, 4098.
- (14) Eisenberg, A. *Macromolecules* **1970**, *3*, 147.
- (15) MacKnight, W. J.; Earnest, J. R. *J. Polym. Sci., Macromol. Rev.* **1981**, *16*, 41.
- (16) Eisenberg, A.; Kim, J. S. *Introduction to Ionomers*; John Wiley & Sons: New York, 1998.
- (17) Hird, B.; Eisenberg, A. *Macromolecules* **1992**, *25*, 6466.
- (18) Moore, R. B.; Cable, K. M.; Croley, T. L. *J. Membr. Sci.* **1992**, *75*, 7.

- (19) Calhoun, B. H.; Moore, R. B. *J. Vinyl Add. Technol.* **1996**, *2*, 358.
- (20) Eisenberg, A.; Yeager, H. L., Eds.; *Perfluorinated Ionomer Membranes*; American Chemical Society: Washington, DC, 1982.
- (21) Cable, K. M.; Moore, R. B. *Polym. Prepr. (Am. Chem. Soc., Div. Polym. Chem.)* **1992**, *33*, 1212.
- (22) Cable, K. M. Ph.D. Dissertation, University of Southern Mississippi, Hattiesburg, MS, 1996.
- (23) Stein, R. S.; Rhodes, M. B. *J. Appl. Phys.* **1960**, *31*, 1873.
- (24) Gierke, T. D.; Munn, G. E.; Wilson, F. C. *J. Polym. Sci., Polym. Phys. Ed.* **1981**, *19*, 1687.
- (25) Lu, X.; Weiss, R. A. *Macromolecules* **1992**, *25*, 6185.
- (26) Eisenberg, A.; Hara, M. *Polym. Eng. Sci.* **1984**, *24*, 1307.
- (27) Register, R. A.; Bell, T. R. *J. Polym. Sci., Part B: Polym. Phys.* **1992**, *30*, 569.
- (28) Tomita, H.; Register, R. A. *Macromolecules* **1993**, *26*, 2796.
- (29) Galambos, A. F.; Stockton, W. B.; Koberstein, J. T.; Sen, A.; Weiss, R. A.; Russell, T. P. *Macromolecules* **1987**, *20*, 3091.
- (30) Fujimura, M.; Hashimoto, T.; Kawai, H. *Macromolecules* **1981**, *14*, 1309.
- (31) Orlor, E. B.; Moore, R. B. *Macromolecules* **1994**, *27*, 4774.
- (32) Hara, M.; Eisenberg, A.; Storey, R. F.; Kennedy, J. P. In *ACS Symposium Series 302*; Eisenberg, A., Bailey, F. E., Eds.; American Chemical Society: Washington, DC, 1986; Chapter 14.
- (33) Weiss, R. A.; Feng, Y.; Tucker, R.; Xie, R.; Han, C. L.; Karim, A. *Soc. Plast. Eng., ANTEC* **1997**, *XLIII*, 2653.
- (34) Lando, J. B.; Olf, H. G.; Peterlin, A. J. *J. Polym. Sci., Part A-1* **1966**, *4*, 941.
- (35) Hasegawa, R.; Takahashi, Y.; Chatani, Y.; Tadokoro, H. *Polym. J.* **1972**, *3*, 600.
- (36) Doll, W. W.; Lando, J. B. *J. Macromol. Sci., Phys.* **1970**, *4*, 309.
- (37) Lovinger, A. J. In *Developments in Crystalline Polymers*; Bassett, D. C., Ed.; Applied Science Publishers: Oxford, 1982; Chapter 5.
- (38) Kawai, H. *Jpn. J. Appl. Phys.* **1969**, *8*, 1975.
- (39) Bergman, J. G., Jr.; McFee, J. H.; Crane, G. R. *Appl. Phys. Lett.* **1971**, *18*, 203.
- (40) Nakamura, K.; Wada, Y. *J. Polym. Sci., Part A-2* **1971**, *9*, 161.
- (41) Doll, W. W.; Lando, J. B. *J. Macromol. Sci., Phys.* **1968**, *2*, 205.
- (42) Matsushige, K.; Nagata, K.; Imada, S.; Takemura, T. *Polymer* **1980**, *21*, 1391.
- (43) Miller, R. L.; Raison, J. *J. Polym. Sci., Polym. Phys. Ed.* **1976**, *14*, 2325.
- (44) Doll, W. W.; Lando, J. B. *J. Macromol. Sci., Phys.* **1970**, *B4*, 889.
- (45) Scheinbeim, J.; Nakafuku, C.; Newman, B. A.; Pae, K. D. *J. Appl. Phys.* **1979**, *50*, 4399.
- (46) Lovinger, A. J. *Polymer* **1981**, *22*, 412.
- (47) Davis, G. T.; McKinney, J. E.; Broadhurst, M. G.; Roth, S. C. *J. Appl. Phys.* **1978**, *49*, 4998.
- (48) Marand, H.; Stein, R. S. *J. Polym. Sci., Polym. Phys. Ed.* **1989**, *27*, 1089.
- (49) Tashiro, K.; Kobayashi, M.; Tadokoro, H. *Macromolecules* **1981**, *14*, 1757.
- (50) Prest, W. M.; Luca, D. J. *J. Appl. Phys.* **1975**, *46*, 4136.
- (51) Kobayashi, M.; Tashiro, K.; Tadokoro, H. *Macromolecules* **1975**, *8*, 158.
- (52) Okuda, K.; Yoshida, T.; Sugita, M.; Asahina, M. *Polym. Lett.* **1967**, *5*, 465.
- (53) Cortilli, G.; Zerbi, G. *Spectrochim. Acta, Part A* **1967**, *23A*, 2216.
- (54) Osaki, S.; Ishida, Y. *J. Polym. Sci., Polym. Phys. Ed.* **1975**, *13*, 1071.
- (55) Starkweather, H. W., Jr. *Macromolecules* **1982**, *15*, 320.
- (56) Lee, H.; Salomon, R. E.; Labes, M. M. *Macromolecules* **1978**, *11*, 171.
- (57) Gal'perin, Y. L.; Kosmynin, B. P.; Smirnov, V. K. *Vysokomol. Soedin., Ser. A* **1970**, *12*, 1880.
- (58) Wang, T. T.; Nishi, T. *Macromolecules* **1977**, *10*, 421.
- (59) Lovinger, A. J. *J. Polym. Sci., Polym. Phys. Ed.* **1980**, *18*, 793.
- (60) Landis, F. A.; Moore, R. B. Manuscript in preparation.
- (61) Martuscelli, E. *Polym. Eng. Sci.* **1984**, *24*, 563.

MA000636A